AD-A179 260 STUDY OF THE INFLUENCE OF METALLURGICAL FACTORS ON FATIGUE AND FRACTURE O..(U) SOUTHWEST RESEARCH INST SAN ANTONIO TX J LANKFORD ET AL. 30 JAN 87 SWRI-06-8972 1/1

UNCLASSIFIED AFOSR-TR-87-0310 F49620-86-C-0024 F/G 11/6 NL

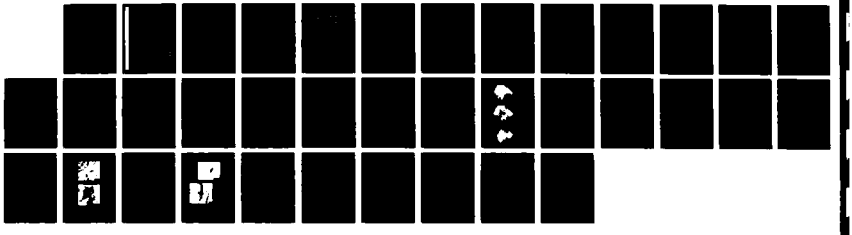

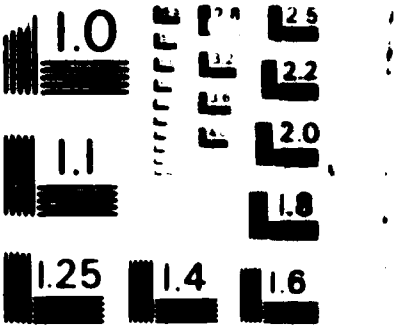
1.0
1.1
1.25
1.4
1.6
1.8
2.0
2.2
2.5

SwRI-8972/1

(2)

STUDY OF THE INFLUENCE OF METALLURGICAL FACTORS ON FATIGUE AND FRACTURE OF AEROSPACE STRUCTURAL MATERIALS

By
James Lankford
David L. Davidson
Kwai S. Chan
Gerald R. Leverant

AFOSR ANNUAL REPORT

This research was sponsored by the Air Force Office of Scientific Research,
Electronic and Materials Sciences Directorate
Under Contract F49620-86-C-0024

Approved for release; distribution unlimited.

January 1987

SOUTHWEST RESEARCH INSTITUTE
SAN ANTONIO HOUSTON

UNCLASSIFIED

SECURITY CLASSIFICATION OF THIS PAGE

REPORT DOCUMENTATION PAGE

1a. REPORT SECURITY CLASSIFICATION UNCLASSIFIED	1b. RESTRICTIVE MARKINGS AD-A179 208
2. SECURITY CLASSIFICATION AUTHORITY	3. DISTRIBUTION / AVAILABILITY OF REPORT Approved for public release; distribution unlimited
2b. DECLASSIFICATION / DOWNGRADING SCHEDULE	
4. PERFORMING ORGANIZATION REPORT NUMBER(S) 06-8972	5. MONITORING ORGANIZATION REPORT NUMBER(S) AFOSR-TR- 87-0310
6a. NAME OF PERFORMING ORGANIZATION Southwest Research Institute	6b. OFFICE SYMBOL (If applicable)
7a. NAME OF MONITORING ORGANIZATION Air Force Office of Scientific Research	
6c. ADDRESS (City, State, and ZIP Code) 6220 Culebra Road San Antonio, TX 78284	7b. ADDRESS (City, State, and ZIP Code) Department of the Air Force Bolling Air Force Base, DC 20332
8a. NAME OF FUNDING / SPONSORING ORGANIZATION AFOSR	8b. OFFICE SYMBOL (If applicable) NE
9. PROCUREMENT INSTRUMENT IDENTIFICATION NUMBER F49620-86-C-0024	
8c. ADDRESS (City, State, and ZIP Code) Department of the Air Force Bolling Air Force Base, DC 20332	10. SOURCE OF FUNDING NUMBERS PROGRAM ELEMENT NO. 61102F; PROJECT NO. 2306; TASK NO. A1; WORK UNIT ACCESSION NO.

11. TITLE (Include Security Classification)
Study of the Influence of Microstructural Factors on Fatigue and Fracture of Aerospace Structural Materials

12. PERSONAL AUTHOR(S)
J. Lankford, D. L. Davidson, G. R. Leverant, K. S. Chan

13a. TYPE OF REPORT	13b. TIME COVERED	14. DATE OF REPORT (Year, Month, Day)	15. PAGE COUNT
Annual Report	FROM 1/1/86 TO 12/31/86	87/1/30	31

16. SUPPLEMENTARY NOTATION

17. COSATI CODES			18. SUBJECT TERMS (Continue on reverse if necessary and identify by block number)
FIELD	GROUP	SUB-GROUP	

19. ABSTRACT (Continue on reverse if necessary and identify by block number)

Aluminum Iron Delta K Delta K sub eff Delta k sub th

This report summarizes the results of a two-phase study involving (1) experimental characterization and analytical modeling of fatigue crack tip micromechanics in aerospace structural (Al) alloys, and (2) identification and modeling of key microstructural factors controlling fracture in Al-(Fe)-X alloys.

Scanning Electron Microscopy

Dynamic load cycling within the (SEM) and stereoimaging strain analysis were used to characterize crack opening loads and crack opening modes for 7091-T7E69 Al alloy. Relationships between (ΔK), (ΔK_{eff}), (ΔK_{th}), and R were defined. These data were used to determine compressive residual stresses within the near crack tip region. It was found that at the

20. DISTRIBUTION / AVAILABILITY OF ABSTRACT	21. ABSTRACT SECURITY CLASSIFICATION
☒ UNCLASSIFIED/UNLIMITED ☐ SAME AS RPT ☐ DTIC USERS	

22a. NAME OF RESPONSIBLE INDIVIDUAL	22b. TELEPHONE (Include Area Code)	22c. OFFICE SYMBOL
Dr A Rosenstein	202-767-4933	NE

DD FORM 1473, 84 MAR — 83 APR edition may be used until exhausted. All other editions are obsolete.

SECURITY CLASSIFICATION OF THIS PAGE

A

cont'd

threshold, crack tips are able to open only in Mode II, i.e., the threshold corresponds to an absence at Mode I crack opening. ~~In addition,~~ a model was developed which relates the threshold stress intensity factor to the length of a microstructure-related dominant slip line length. The validity of the model was tested experimentally, with reasonable agreement between predicted and measured results.

The fracture behavior of Al-Fe-X alloys was investigated with the objectives of identifying the micromechanisms of fracture and establishing microstructure/property relationships in this series of dispersoid-strengthened, powder-metallurgy aluminum alloys. ~~In particular,~~ tensile and fracture toughness tests were performed at room temperature to obtain the yield stress (σ_y), strain hardening exponent (n), the local fracture strain (ε_f^*), and the critical stress intensity at fracture (K_{Ic}). ~~In addition,~~ the size distribution and volume fraction of dispersoids were characterized using quantitative light and electron microscopies. Preliminary results indicated that the K_{Ic} value of the extruded Al alloys is in the range of 5-10 MPa$\sqrt{m}$. The K_{Ic} values increase with increasing values of $n\sqrt{E\sigma_y}$, but decrease with ε_f^*. Correlations of the K_{Ic} value with fractographic observations and dispersoid size measurements revealed that fracture of the Al-Fe-X alloys might be controlled by cavity nucleation at 0.1-1 μm diameter dispersoids, and possibly by fracture at prior powder particle boundaries in one of the alloys.

B

SOUTHWEST RESEARCH INSTITUTE
Post Office Drawer 28510, 6220 Culebra Road
San Antonio, Texas 78284

STUDY OF THE INFLUENCE OF METALLURGICAL FACTORS ON FATIGUE AND FRACTURE OF AEROSPACE STRUCTURAL MATERIALS

By
James Lankford
David L. Davidson
Kwai S. Chan
Gerald R. Leverant

AFOSR ANNUAL REPORT

This research was sponsored by the Air Force Office of Scientific Research,
Electronic and Materials Sciences Directorate
Under Contract F49620-86-C-0024

Approved for release; distribution unlimited.

January 1987

Approved for public release;
distribution unlimited.

Approved:

U. S. Lindholm, Vice President
Engineering and Materials Sciences Division

I. RESEARCH OBJECTIVES

A. Task 1. Crack Tip Micromechanisms and Fatigue Lifetime Prediction

1. Perform detailed measurements and analysis of fatigue crack closure.

2. Investigate ways of including this information in models for fatigue crack growth.

B. Task 2. Microstructure/Property Relationships in Advanced Structural Alloys

1. Develop an understanding of the microstructure/property relationships in advanced Al-Fe-X alloys.

2. Identify the micromechanisms of fracture in dispersoid-hardened, powder-metallurgy Al alloys.

3. Devise a procedure for enhancing fracture toughness through microstructure modifications.

II. STATUS OF THE RESEARCH EFFORT

A. Task 1. Crack Tip Micromechanisms and Fatigue Lifetime Prediction

1. Scope

The principal thrust of the aluminum task has been to understand in detail how fatigue cracks grow, including the influence of microstructure. Past effort on this contract has included measurement of crack tip parameters and the derivation of models using this information to describe fatigue crack growth. To date, crack closure has not been incorporated in the modeling process because no fundamental understanding of its origin has been available. But, as many investigations have discovered, fatigue crack closure is a very important part of understanding fatigue crack growth. Thus, the focus of the past year's work has been on gaining a better understanding of crack closure and how to include it in the modeling of incremental crack advance. Work on this problem is still underway, but the status at this time is summarized in this section.

2. Current Status

a. Crack Closure

While plasticity at the crack tip is the fundamental factor in determining fatigue crack growth, it is also an important element in crack closure, which inhibits crack growth. One way to envision the complex interaction of the various factors important to crack growth is shown in Fig. 1.

As shown in the figure, closure is not only caused by plasticity, but also by other mechanisms mainly related to environment, such as oxide induced closure. Not shown specifically on the diagram is the possible mechanism of roughness induced crack closure, although it could be included in the plasticity term. The effect of all these closure mechanisms is to decrease the applied driving force, ΔK. Thus, crack tip plasticity has two opposing effects: while it is the cause of fatigue crack growth, it also lowers the applied stress intensity factor.

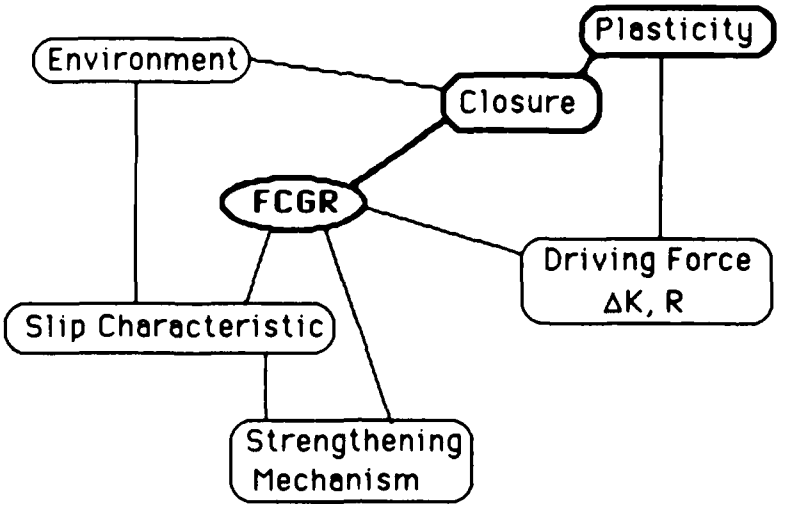

Figure 1. Schematic representation of the various factors affecting fatigue crack growth rate (FCGR). Plasticity, closure and their relation to crack growth are highlighted.

Our detailed work on closure has involved the powder metallurgy aluminum alloy 7091-T7E69, a material for which we have previously made detailed measurements of crack tip parameters [1] and done microstructural characterization, modeling [2], and analysis of the crack growth process [3]. Full results of the closure analysis were reported at the ASTM Crack Closure Symposium, May 1986, and will be published in the Proceedings volume [4,5]. The following summary highlights only a few of the findings of this work.

Analyses of partially and fully loaded fatigue cracks at $R = 0.1$, 0.4, and 0.8, and for cyclic stress intensities of $\Delta K = 4$, 6 and 10 MPa$\sqrt{m}$, were made using the stereoimaging technique under conditions in which environment had very little influence. Thus, plasticity should have been the predominant mechanism of crack closure. The alloy studied had a very small grain size, which resulted in a fracture surface of limited topography, thereby reducing roughness induced closure to a minimum.

Peeling open of the cracks with increasing load was monitored, and careful measurements of crack opening load were made, mainly using a cyclic loading stage for the scanning electron microscope together with stereoimaging, in order to obtain the spatial resolution offered by that method. It was found that there were, in fact, two values of opening load, one for Mode I and another for Mode II. The ratio of these two opening loads depends on both ΔK and R, as is shown in Fig. 2; this format for displaying the data is used in the figure because other work [4] has shown that this format yields a linear relation between U and $1/\Delta K$ at $R = 0.1$, and between U and $1/K_{max}$ for $R < 1$, for Mode I. To date, this relation has been shown to describe closure in both 7091 aluminum alloy and 304 stainless steel. At $R = 0.1$, $\Delta K = 10$ MPa$\sqrt{m}$, the effective ΔK for both crack opening modes is about the same, but with decreasing ΔK, U for Mode II is larger than that for Mode I. When $U = 0$, $\Delta K_{eff} = 0$, which may be interpreted as being that value of ΔK for which the crack would stop growing (ΔK_{th}) if the crack tip were responding by a purely Mode I opening. But, as found previously [6], fatigue cracks open with an increasing amount of Mode II as ΔK is decreased. This trend may be extrapolated to indicate that at the threshold for crack growth, the crack is opening only

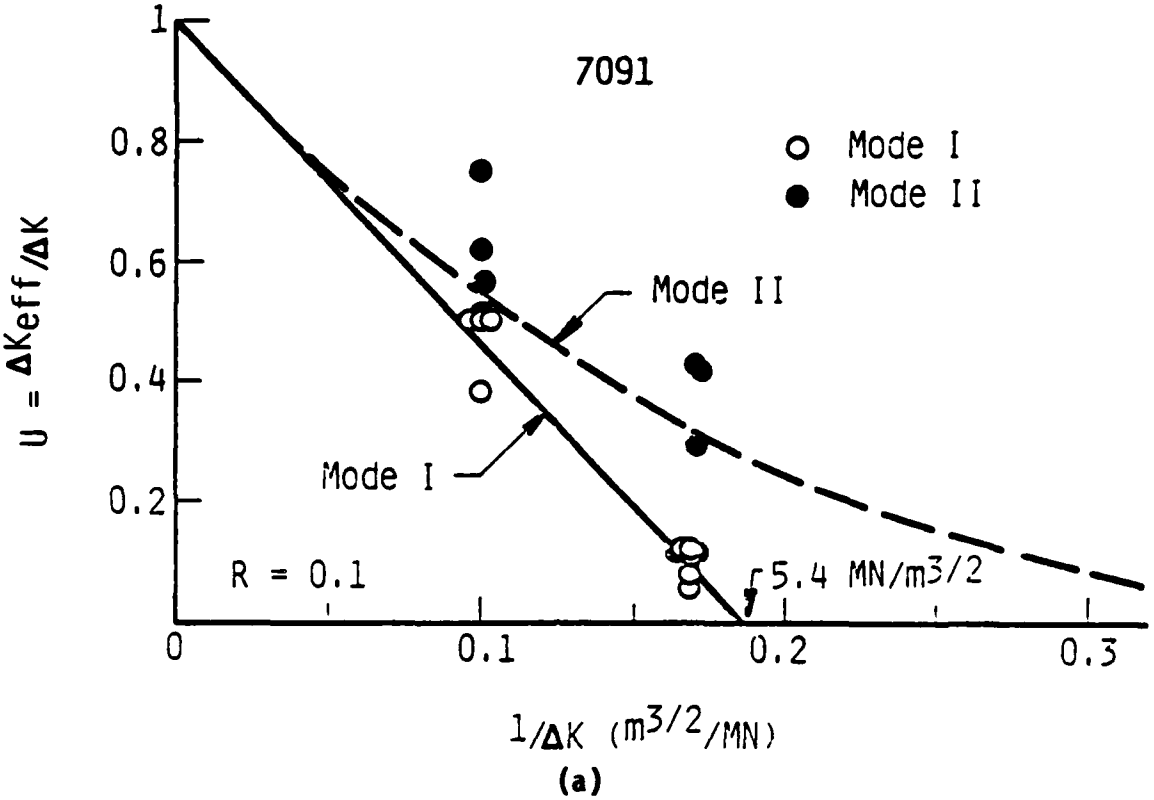

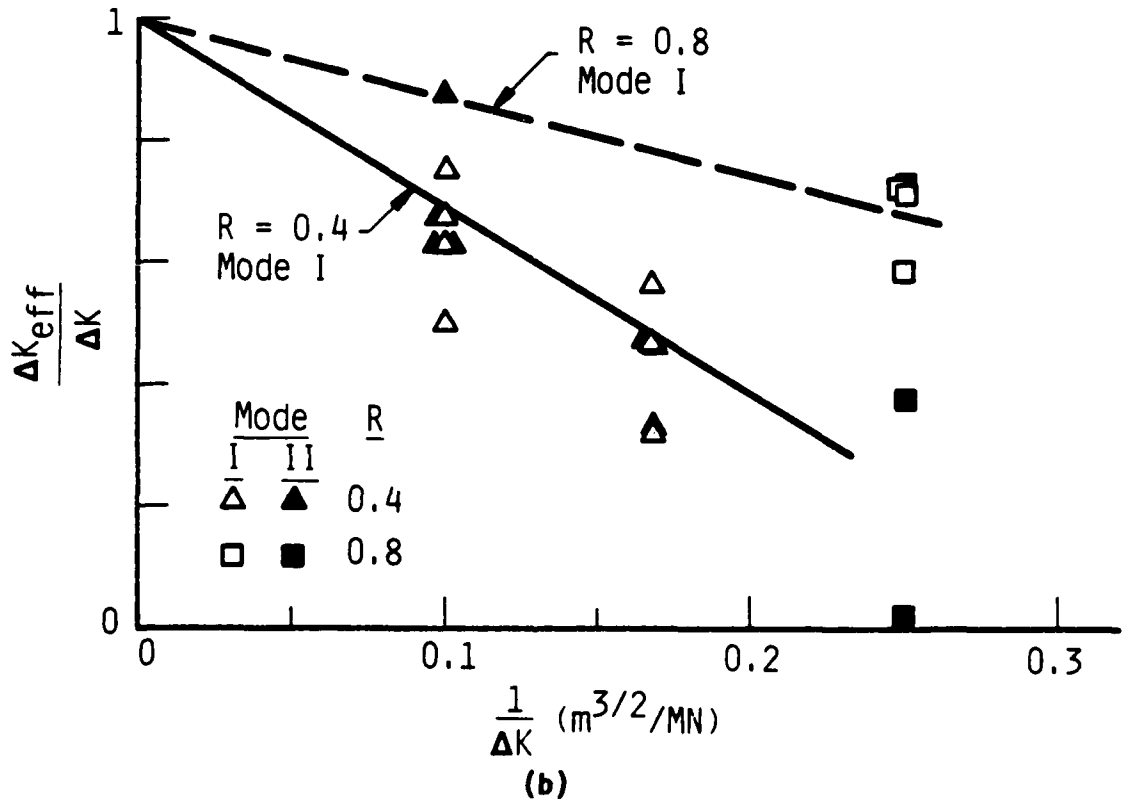

Figure 2. (a) ΔK_{eff} for R = 0.1.
(b) ΔK_{eff} for R = 0.4 and 0.8.

in Mode II. In fact, this investigation found that cracks could grow by exhibiting only Mode II opening, with Mode I so small that it was not measurable.

The relation for Mode I crack opening shown in Fig. 2 is

$$U = \Delta K_{eff}/\Delta K = 1 - \Delta K^0/\Delta K \qquad (1)$$

where ΔK^0 is considered to be the Mode I value of ΔK_{th}. In this relation ΔK_{eff} is defined as K_{max}-K_{open}, but by setting $\Delta K^0 = \Delta K_{th}$, ΔK_{eff} may be also defined as

$$\Delta K_{eff} = \Delta K - \Delta K_{th} \qquad (2)$$

Thus, if ΔK_{th} can be determined, then for any applied ΔK, a value of Mode I K_{open} may be computed.

High resolution determination of crack opening as a function of increasing load shows that the relation is highly non-linear, Fig. 3(a). The information in this curve may be used to derive the residual stresses within the near crack tip region by using an analysis due to Fleck [7]. Stresses so derived for ΔK = 6 MPa$\sqrt{m}$, R = 0.1, are shown in Fig. 3(b). Maximum values of compressive residual stress at the crack tip computed by this analysis are approximately twice the tensile yield stress, as might be expected from Rice's analysis of crack tip plasticity. The low work hardening coefficient for aluminum alloys is not too different from Rice's assumption of no work hardening (elastic-perfectly plastic material).

Likewise, residual plasticity in the wake of the crack has been measured, Fig. 4. Most of the elongation in material near the crack is found within a region of width D_R = 3 μm, as shown on the figure. The net residual elongation in the loading direction averaged 0.3 μm for this crack. The closure measured for this loading level, ΔK = 6 MPa$\sqrt{m}$, R = 0.1, must be due either to residual wake plasticity or the residual stress attending the crack tip, or both, but a method of relating these factors to compute crack closure has not yet been found. A strip-yield

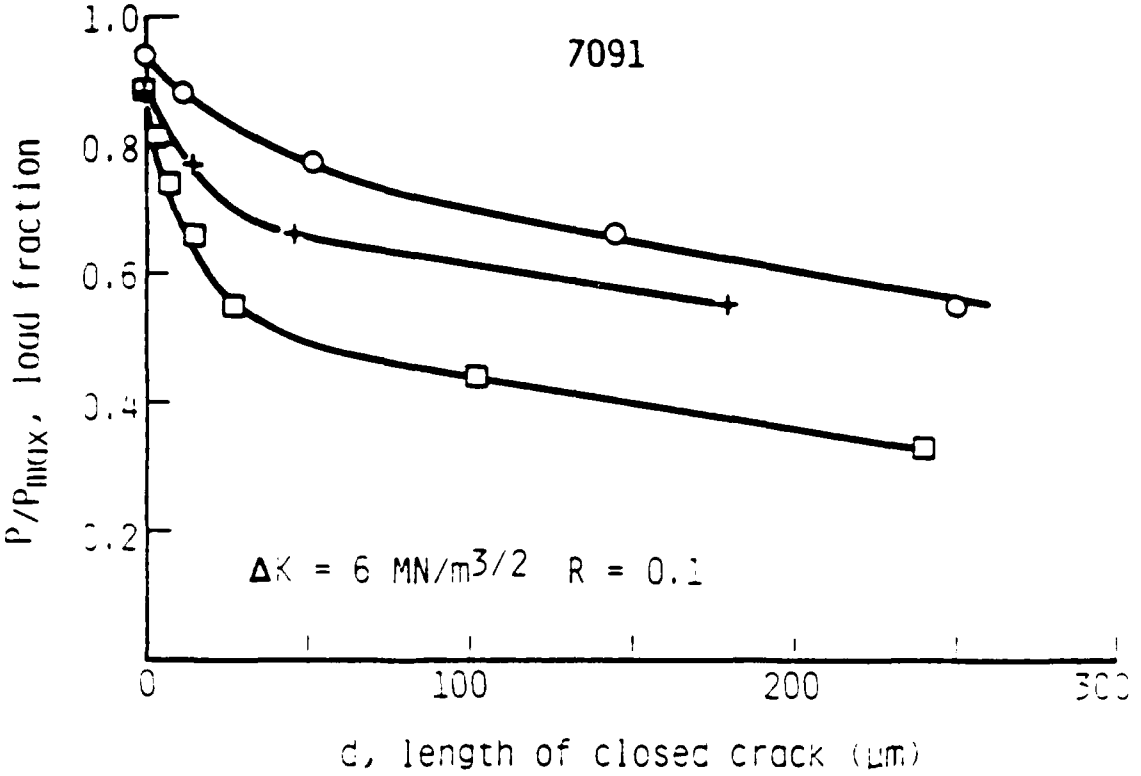

Figure 3a. The length of closed crack as a function of load. $\Delta K = 6\ MN/m^{3/2}$, R = 0.1. Different symbols denote different experiments, but on the same specimens.

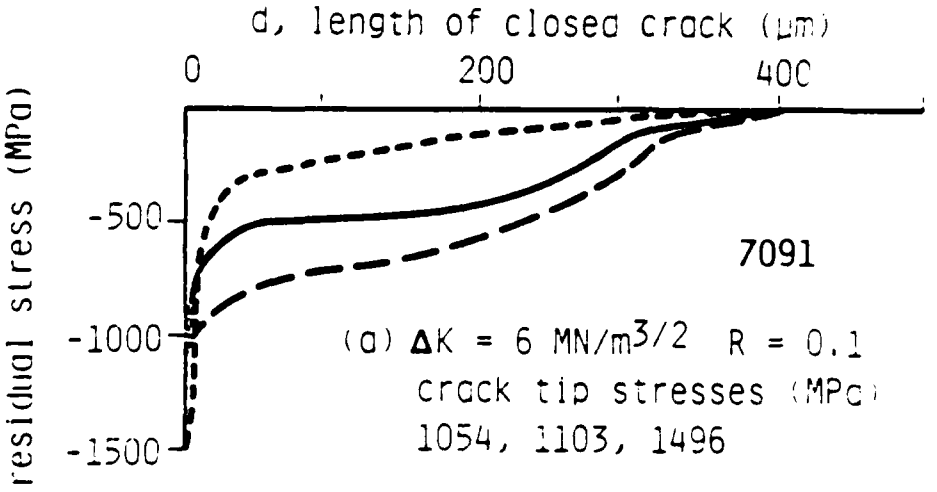

Figure 3b. Residual stresses along the crack flank computed from the opening load using Fleck's Analysis.

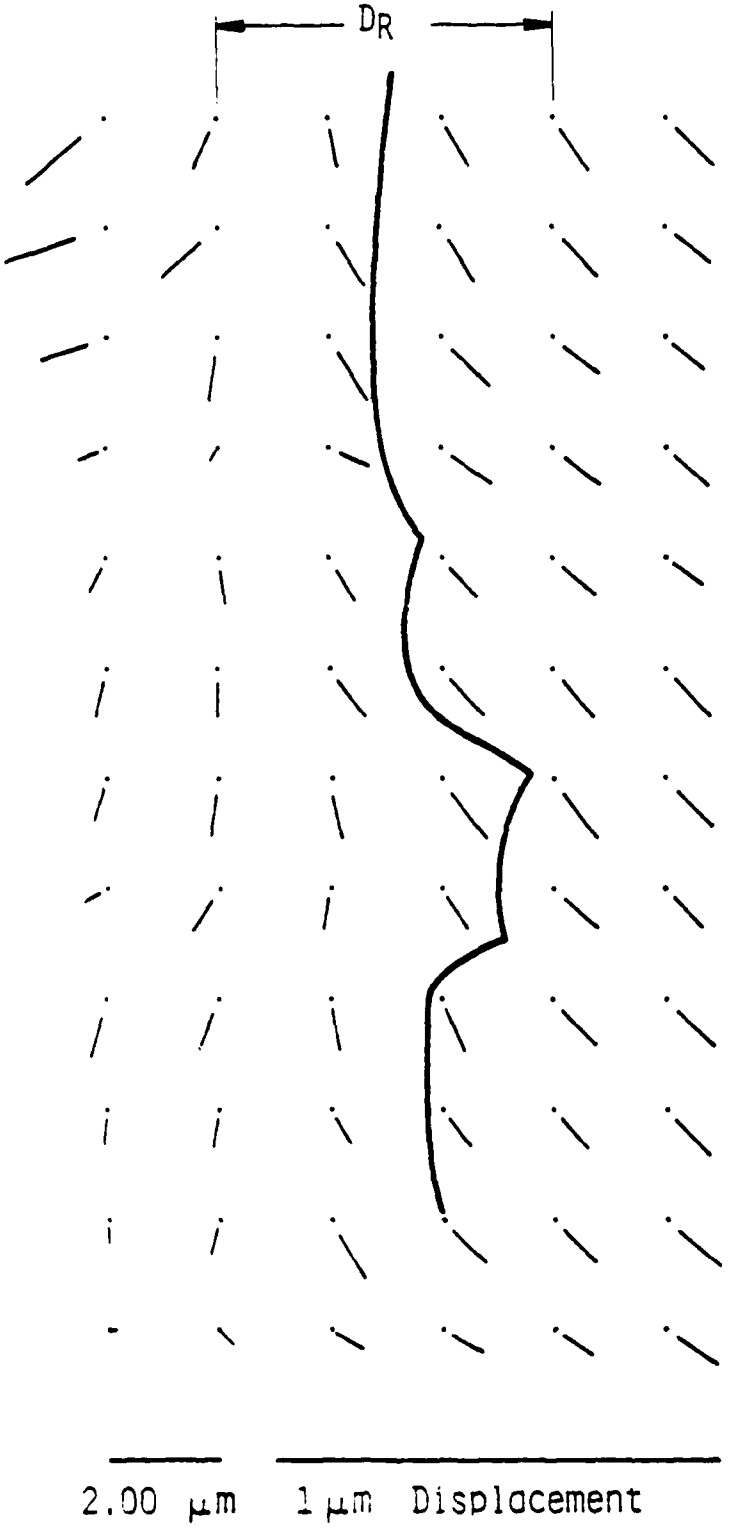

Figure 4. Net displacements caused by growth of a fatigue crack at $\Delta K = 6$ $MN/m^{3/2}$, $R = 0.16$. Note that the displacements shown are enlarged (scale on right) relative to the spatial scale (on left). A dot marks the original position of the material point, and the end of the line is the point to which the material has been displaced by passage of the crack. The reference point from which these displacements were measured was located in material undisturbed by the crack, approximately 20 μm ahead of the tip.

model of the type used by Newman [8] and Fuhring and Seeger [9] may allow these factors to be combined, and this possibility is being explored.

b. Crack Tip Yielding

It was found that plastic flow occurs at fatigue crack tips prior to Mode I opening, for R = 0.1, $6 < \Delta K < 10$ MPa$\sqrt{m}$, which is not surprising considering the amount of Mode II opening which accompanies such cracks. Over the limited range studied, increasing ΔK caused the maximum strain at the crack tip to be increased, but not the strain at crack opening load. These findings are still being analyzed.

The shift in mode mix with decreasing ΔK found in this work and a previous experimental program [1], together with the development of a model for fatigue crack growth [10], has led to another concept related to the threshold for fatigue crack growth at low R ratio. Model formulation led to the idea of a microstructurally defined slip parameter which was related to crack opening displacement and crack tip strain. The model also indicated that near the threshold ΔK, only one slip line extended ahead of the crack tip at a small angle to the direction of growth. This geometric relationship is shown in Fig. 5 along with the measured strain distribution [11] accompanying the crack. The stress distribution shown was not measured, but is compatible with the actual strain distribution. The assumption made is that at this very low value of ΔK, the plastic zone size ahead of the crack has diminished to that caused by the dominant slip line of length r_s, so that the stress distribution attending a linear elastic crack is valid outside this zone, and may be used to compute the stress intensity factor, according to the following equation:

$$\Delta K_{th} = \sigma_y \sqrt{2\pi r_s} \qquad (3)$$

where σ_y is the yield stress (or perhaps the proportional limit stress).

This concept may be used in two ways: If ΔK_{th} is known, then r_s, the microstructural parameter, may be computed; or conversely, if r_s is known, then ΔK_{th} may be determined. Table 1 shows values values of ΔK_{th} computed using Eq. (3) and the values of r_s previously derived

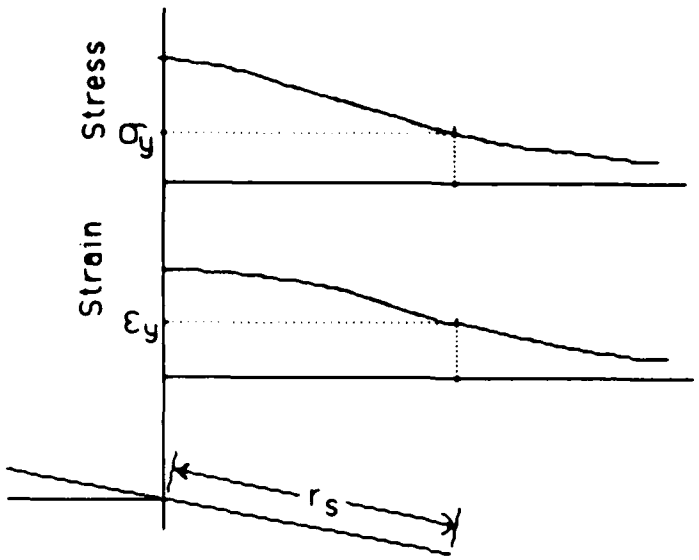

Figure 5. Schematic representation of a fatigue crack growing just above the threshold ΔK, which has a slip line of length r_s emanating from its tip. The distributions of stress and strain are also shown, with elastic values of each at the distance r_s from the crack tip.

[2,12] for the alloys studied. Computed values of ΔK_{th} agree reasonably well with those measured, considering the uncertainties in yield stress and r_s, and in measured ΔK_{th}.

TABLE 1

Material	Yield Stress MPa	r_s μm	ΔK_{th} Derived MPa	ΔK_{th} Measured MPa
7075-T651	508	5 ± 2	2.2-3.3	1.5-3
7091-T7E69	503	5 ± 2	2.2-3.3	1.7 vac 3.5 air
Ti-6Al-4V	862	4.5 ± 1	4-5	1.6 vac 7.7 air

Another way to derive a value of the microstructural parameter r_s is to use the crack tip strain together with the strain distribution within the plastic zone measured at higher values of ΔK. If the same distribution of strain is assumed to be valid at ΔK_{th}, even though the mode mix has changed, then it is possible to use the same concept as shown in Fig. 5 to derive a value of either r_s or ΔK_{th}, assuming that the strain is elastic at the end of the slip line.

It should be possible to derive an effective ΔK at the crack tip from measured changes in crack opening displacement, COD, with distance behind the crack tip, y. For an elastic crack, COD should vary as $\sqrt{y}$, and ΔK should be directly proportional to the ratio COD/$\sqrt{y}$. It has been found for most of the cracks examined to date that COD plotted vs $\sqrt{y}$ does yield a constant slope from which K may be computed. When this value of K, termed Ke, is plotted vs the crack tip strain, much of the scatter in this correlation found when the applied ΔK was used [1,12] is eliminated. This is shown for 7075-T651 in Fig. 6. The correlation shown may be expressed as

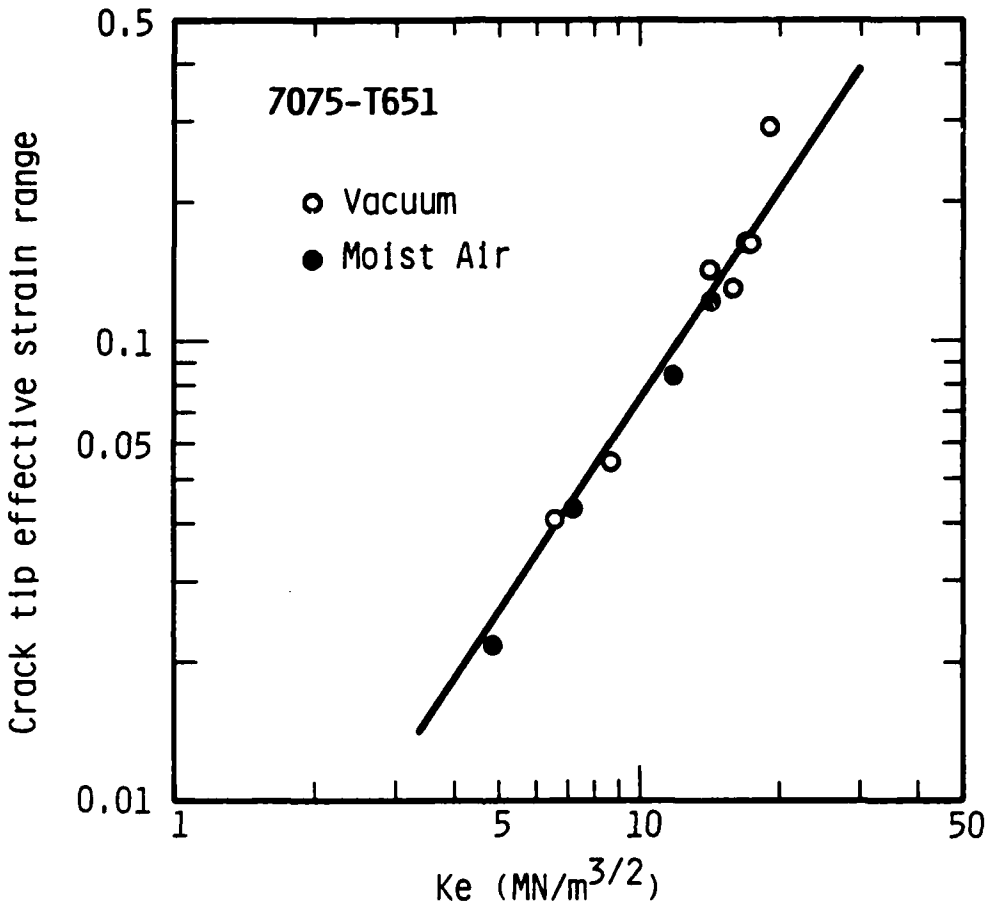

Figure 6. Crack tip strain vs K as derived from COD vs$\sqrt{y}$ analysis.

$$\text{Crack tip strain} = \Delta\varepsilon(0) = K_o Ke^r \qquad (4)$$

Near the threshold ΔK, Ke should be a small value: Ke = 1-2 MPa$\sqrt{m}$; thus it is should possible to compute crack tip strain near the threshold and relate the measured distribution of strain, the parameter r_s, and the elastic strain as another check on the concept expressed by Eq. (3).

From Ref. [11], strain distributions within the plastic zones of fatigue cracks at low R ratio were best described by the following expression

$$\varepsilon(r)/\Delta\varepsilon(0) = \varepsilon' = A' - M' \ln(r+B) \qquad (5)$$

where A', M' and B are all factors derived from the measured strain distribution.

The procedure used to relate the factors described above is as follows: from yield stress and modulus the elastic strain is calculated; using values of r_s given in Table 1 and the values of A', M' and B given in [11], a value of crack tip strain may be computed; this value of $\Delta\varepsilon(0)$ is then used in Eq. (4) to compute the value of Ke. The values of Ke derived using this procedure are shown in Table 2.

TABLE 2

Material	K_o	r	Ke (derived) MPa$\sqrt{m}$
7075-T651	2.3×10^{-3}	1.48	2.1
Ti-6Al-4V	8×10^{-4}	1.46	5.1
7091-T7E69	1.3×10^{-2}	1.07	0.9

These values are not as close as desired (1-2 MPa$\sqrt{m}$), but considering the extrapolations and assumptions used, the results are considered to be reasonable.

c. Summary

This study has shown that fundamental relationships useful in the understanding of the fatigue crack growth process may be derived at near-threshold values of ΔK. These results indicate that it may be possible to predict ΔK_{th} from crack closure data measured at higher ΔK. This has practical value because it may help in the formulation of future alloy compositions and in the assessment of fatigue properties of future materials. At the threshold, the model allows all of the factors discussed above to be related to the basic value of the growth increment, i.e., the striation spacing. These interrelationships are shown schematically in Fig. 1.

A current assessment of the physics relevant to fatigue crack growth is as follows: the threshold for crack growth is reached when the stress at the end of the slip line is elastic, thereby allowing only a limited number of dislocations to be released from the crack tip. The growth increment is the displacement along this slip line caused by the dislocations on it, and that is also the crack opening displacement, which is nearly all Mode II. The microstructural elements which permit this combination of events are fixed at the threshold and continue to control the growth of the crack as ΔK is increased, with the growth increment being modified accordingly. This prediction may be checked by measuring the variation in striation spacing with increasing ΔK.

3. References

[1] D. L. Davidson and J. Lankford, "Fatigue Crack Tip Mechanics of a Powder Metallurgy Aluminum Alloy in Humid Air", Fatigue of Engineering Materials and Structures, 7, 29-39 (1984).

[2] D. L. Davidson and J. Lankford, "The Effects of Aluminum Alloy Microstructure on Fatigue Crack Growth", Materials Science and Engineering, 74, 189-199 (1985).

[3] D. L. Davidson and J. Lankford, "The Breakdown of Crack Tip Microstructure During Fatigue Crack Extension in Aluminum Alloys", in High Strength Powder Metallurgy Aluminum Alloys - II, G. J. Hildeman and M. J. Koczak, eds., TMS-AIME, Warrenville, PA, 1986, pp. 47-59.

[4] S. J. Hudak, Jr. and D. L. Davidson, "Local Crack Tip Opening Load and Its Dependence on Fatigue Loading Variables", ASTM Conference on Fatigue Crack Closure.

[5] D. L. Davidson, "Plasticity Induced Fatigue Crack Closure", ASTM Conference on Fatigue Crack Closure.

[6] D. L. Davidson and J. Lankford, "Mixed Mode Crack Opening in Fatigue", Materials Science and Engineering, 60, 225-229 (1983).

[7] N. A. Fleck, "An Investigation of Fatigue Crack Closure", Ph.D. Dissertation, Cambridge University, May 1984, pp. 109-113.

[8] J. C. Newman, "A Crack-Closure Model for Predicting Fatigue Crack Growth Under Aircraft Spectrum Loading", ASTM STP 748, 1981, pp. 53-84.

[9] H. Fuhring and T. Seeger, "Dugdale Crack Closure Analysis of Fatigue Cracks Under Constant Amplitude Loading", Engineering Fracture Mechanics, 11, 99-122 (1979).

[10] D. L. Davidson, "A Model for Fatigue Crack Advance Based on Crack Tip Metallurgical and Mechanics Parameters", Acta Metallurgica, 32, 707-714 (1984).

[11] D. L. Davidson, "The Distribution of Strain Within Crack Tip Plastic Zones", Engineering Fracture Mechanics, 25, 123-132 (1986).

[12] D. L. Davidson and J. Lankford, "Fatigue Crack Growth Mechanics for Ti-6Al-4V (RA) in Vacuum and Humid Air", Metallurgical Transactions A, 15A, 1931-1940 (1984).

B. Task 2. Microstructure/Property Relationships in Advanced Structural Alloys

1. Scope

Recent advances in alloy development and processing techniques have produced a new family of aluminum alloys, Al-Fe-X, which may be suitable for structural applications at service temperatures up to 340°C. Hardened by a high volume fraction of thermally stable dispersoids, the Al-Fe-X alloys show good strength, high creep resistance, and adequate to moderate ductility at both room and elevated temperatures [1]. Unfortunately, the plane strain toughness of these alloys is low ($\leq$ 10 MPa$\sqrt{m}$) [1] and must be increased considerably before structural uses of large extruded parts are feasible. The current program is aimed at improving the fracture toughness of Al-Fe-X alloys by developing a fundamental understanding of the fracture mechanisms in these dispersoid-hardened alloys. The efforts of the program are focused on (1) establishing microstructure/toughness relationships, (2) identifying origins of low fracture toughness, and (3) developing means for toughness enhancement of Al-Fe-X alloys.

2. Current Status

Three state-of-the-art Al-Fe-X alloys of interest to the Air Force were selected for studies. The alloys selected and their manufacturers include: (1) Al-8Fe-7Ce (Alcoa), (2) Al-8Fe-2Mo-1V (Pratt & Whitney Aircraft), and (3) Al-10.5Fe-2.5V (Allied-Signal). All three alloys were supplied by Lockheed-California Company. The efforts to date will be discussed as follow: (a) characterization of microstructure, (b) characterization of tensile properties, (c) fracture toughness results, (d) fractographic observations, and (e) discussion on toughness enhancement and future work.

a. Microstructures

Optical and transmission electron microscopies were used to characterize the microstructures of the powder-metallurgy Al-Fe-X alloys. Results of optical microscopy, shown in Fig. 1, reveal that Al-8Fe-7Ce contains a relatively high volume fraction of light, featureless

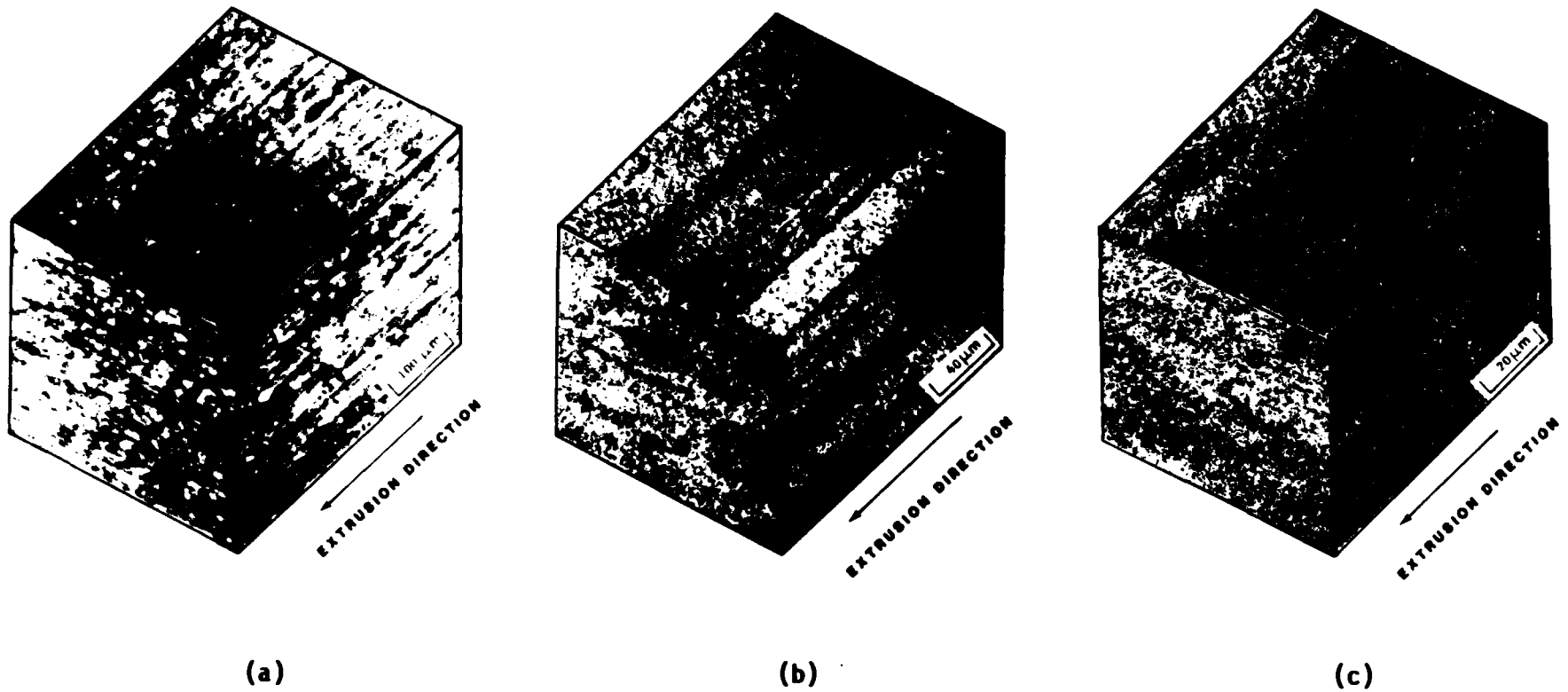

Figure 1. Microstructures of powder-metallurgy Al-Fe-X alloys: (a) Al-8Fe-7CE, (b) Al-8Fe-2Mo-V, and (c) Al-10.5Fe-2.5V.

Zone A particles [2], as well as small, dark intermetallic dispersoids (Fig. 1a). The microstructures of Al-8Fe-2Mo-1V and Al-10.5Fe-2.5V consist primarily of intermetallic dispersoids, while the latter also contains isolated as well as stringer inclusions.

The presence of Zone A particles and small dispersoids in Al-Fe-X alloys provides potential sites for cavity nucleation. To establish the influence of these particles on fracture toughness, the size and distribution of Zone A particles and intermetallic dispersoids were determined by quantitative metallography using TEM photographs of either thin foils or replicas and a Dapple image analysis system. Figure 2a shows that the diameter of the Zone A particles in Al-Fe-Ce is in the range of 1-10 μm, with a total volume fraction of 13%. In comparison, the dispersoids in Al-8Fe-2Mo-1V, which are probably $Al_{12}Fe(Mo,V)$ and Al_6Fe [3], exhibit a size range of 0.1-2 μm diameter and a total volume fraction of 17% (Fig. 2b). Efforts are currently underway to characterize the size distribution of dispersoids in the other alloys.

b. Characterization of Tensile Properties

Tensile tests were performed on 1-mm thick sheet specimens at ambient temperature at strain rates of $1x10^{-3}$ and $1x10^{-5}sec^{-1}$. Typical stress-strain curves shown in Fig. 3 indicate that Al-10.5Fe-2.5V exhibits the highest strength, followed by Al-8Fe-7Ce and Al-8Fe-2Mo-1V. The strain hardening exponents of the three alloys are, however, in the reverse order. The plastic flow behavior of the Al-Fe-X alloys is considerably more rate-sensitive than conventional Al alloys, for which the m values are generally zero or negative. Summary of uniaxial tensile data of the Al-Fe-X alloys is shown in Table 1.

All the tensile specimens were gridded with regularly spaced lines of 1.27 mm spacing and circles of 0.5 mm diameter. The gridded specimens allowed determination of the strain distribution along the gauge length of the specimens and the local strain at the onset of fracture. Figure 4 shows comparison of the strain distributions as a

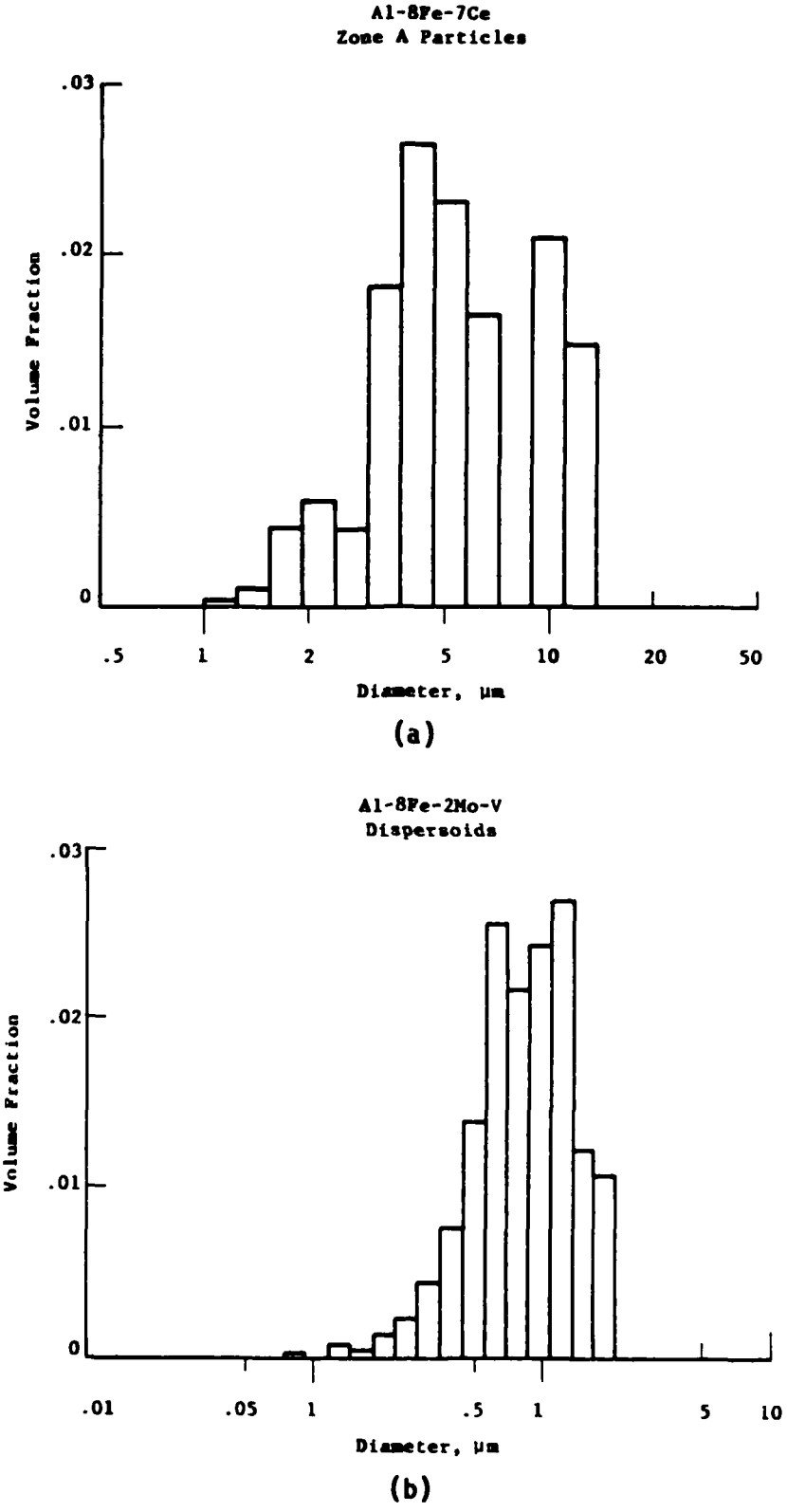

Figure 2. Particle size distribution in Al-Fe-X alloys: (a) Zone A particles in Al-8Fe-7Ce, and (b) intermetallic dispersoids in Al-8Fe-2Mo-V.

TABLE 1

SUMMARY OF TENSILE AND FRACTURE PROPERTIES OF Al-Fe-X ALLOYS

Materials	σ_y, MPa	σ_{uts}, MPa	E, MPa	m	n	ε_u, %	ε_f^*, %	K_{Ic}, MPa$\sqrt{m}$
Al-8Fe-7Ce	418.9	484.9	8.1×10^4	.0166	.053	2.8	15	8.46
Al-8Fe-2Mo-1V	323.5	406.6	8.0×10^4	.0152	.084	3.6	18	9.02
Al-10.5Fe-2.5V	464.1	524.5	8.9×10^4	.0218	.036	1.9	8	5.72

$n = d \log\sigma / d \log\varepsilon^p$

$m = d \log\sigma / d \log\dot{\varepsilon}$

*Local fracture strain measured by the photogrid technique.

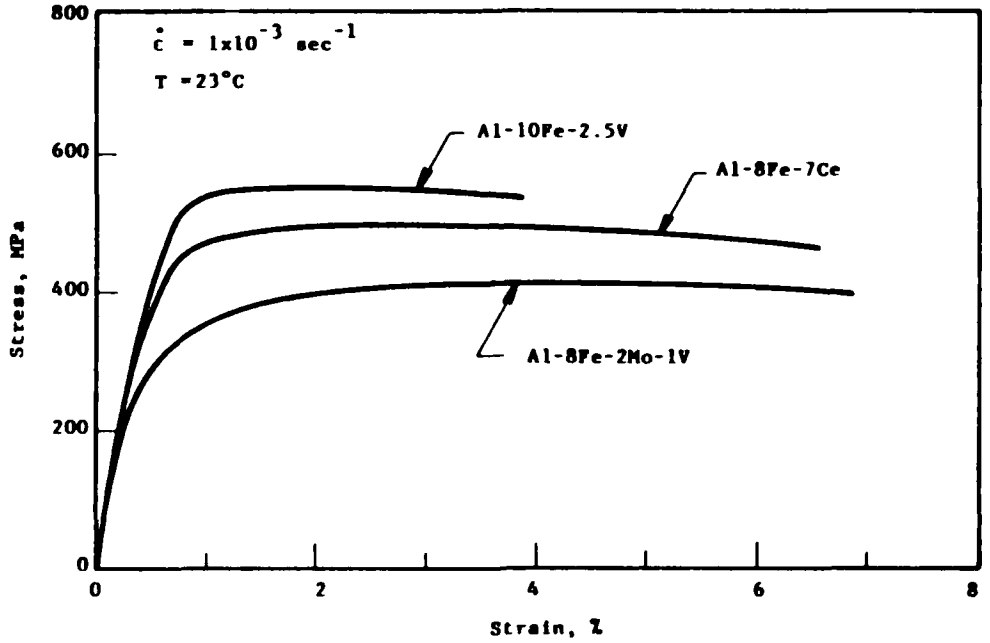

Figure 3. Stress-strain curves of Al-Fe-X alloys.

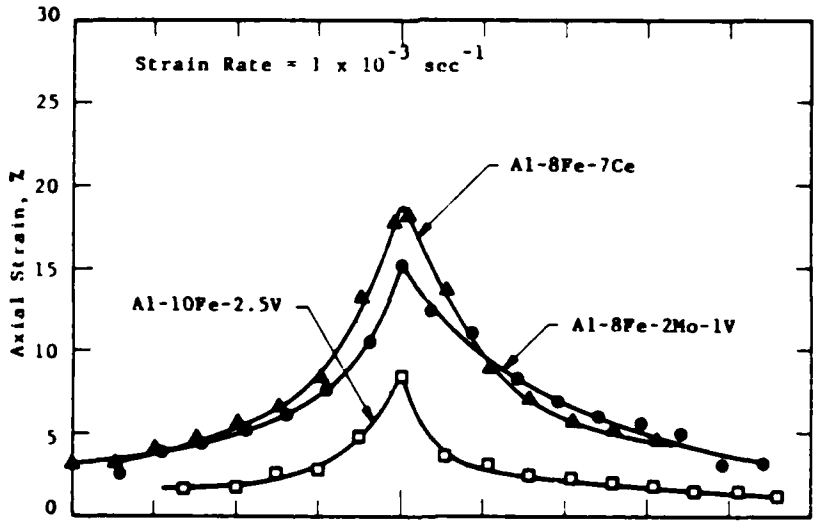

Figure 4. Axial strain as a function of distance from the fracture surface in tensile specimens of Al-Fe-X alloys.

function of distance from the fracture surface. Note that the local fracture strain for Al-10.5Fe-2.5V is 8%, compared to ≈ 17% for Al-8Fe-7Ce and Al-8Fe-2Mo-1V.

c. Fracture Toughness Results

The fracture toughness of the Al-Fe-X alloys was characterized by testing compact-tension specimens. The dimensions of the specimens meet all the requirements specified in the ASTM E399 standard [4]. The specimen thickness was either 3.2 or 10.2 mm. Both the LT and the TL orientations were tested. All the fracture specimens were fatigued precracked and tested at ambient temperature.

Figure 5 summarizes the fracture toughness results of the present program with previous data obtained by Lockheed [3]. The two sets of data are in good agreement. Figure 5 indicates that the K_{Ic} values of Al-8Fe-7Ce and Al-8Fe-2Mo-1V are in the 8-10 MPa$\sqrt{m}$ range, while it is ≈ 5 MPa$\sqrt{m}$ for Al-10.5Fe-2.5V. In addition, the K_c values increase with decreasing specimen thickness, and are practically identical in the TL and LT orientations. Correlation of the tensile properties with toughness results revealed that K_{Ic} increases with the local fracture strain. Furthermore, the K_{Ic} values of the Al-Fe-X alloys increase with $n\sqrt{E\sigma_y}$, a behavior also observed in other Al alloys [5,6].

d. Fractographic Observations

Scanning electron microscopy was used to characterize the fracture surfaces of both the uniaxial tensile and CT specimens. In Al-8Fe-2Mo-1V and Al-10.5Fe-2.5V, fracture of tensile specimens initiated at 50 μm particles which were identified by EDS and Auger spectroscopy to be Al-Fe intermetallic particles containing more Fe than the matrix. Fracture initiation at Al-Fe intermetallic particles was not observed in the CT specimens.

Both the tensile and fracture toughness specimens of the Al-Fe-X alloys exhibit fracture surfaces which are covered with small dimples but give a "lumpy" appearance, as illustrated in Fig. 6 for Al-8Fe-7Ce. The "lumpy" appearance in the Al-Fe-Ce alloy appears to be the consequence of fracture near (but not necessary along) the interface of

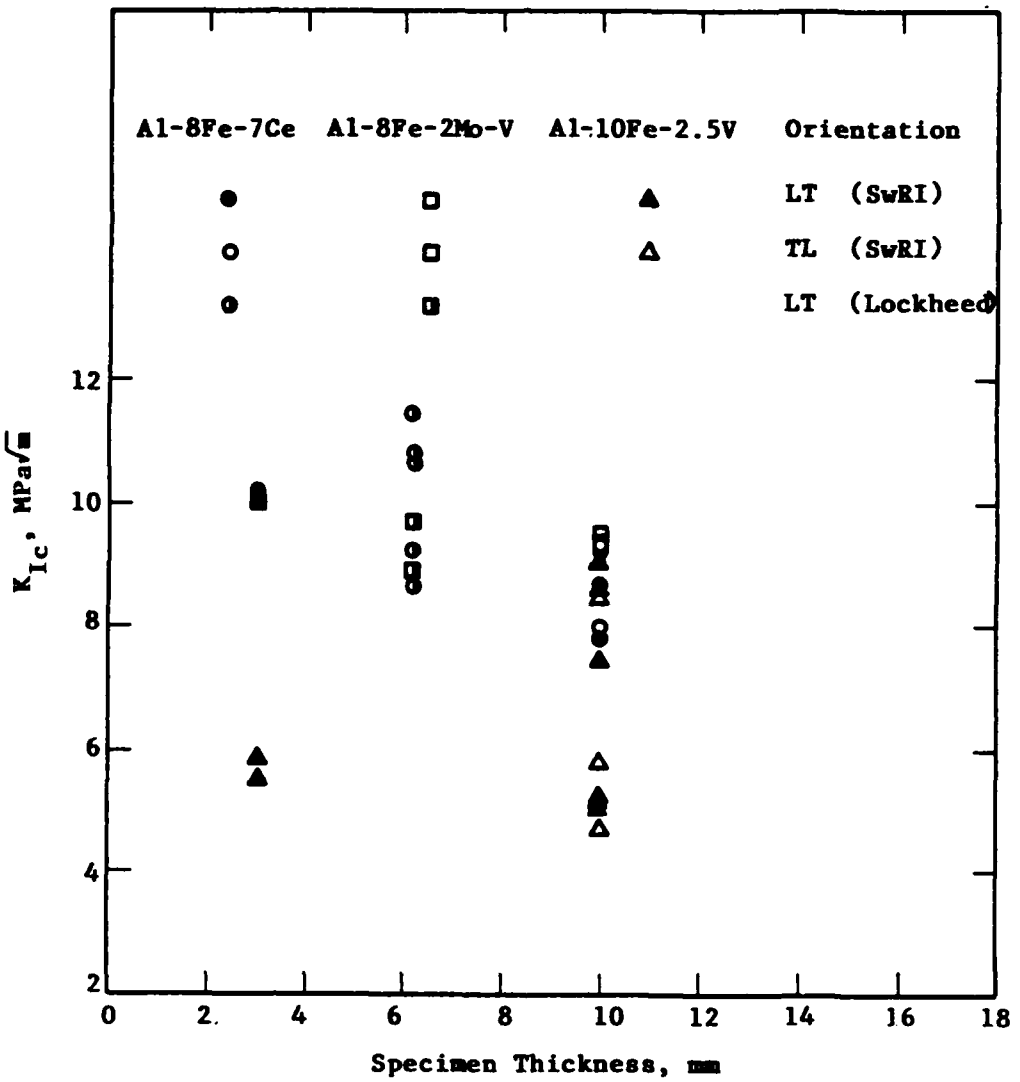

Figure 5. Fracture toughness values of Al-Fe-X alloys as a function of specimen thickness.

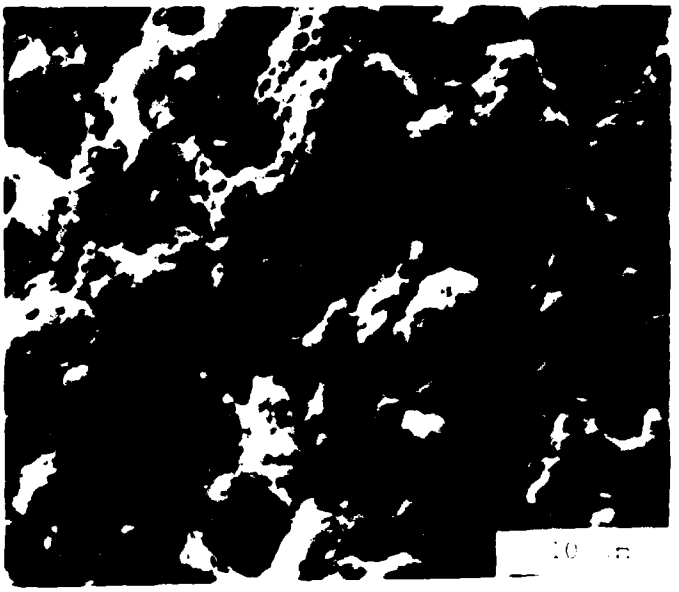

(a)

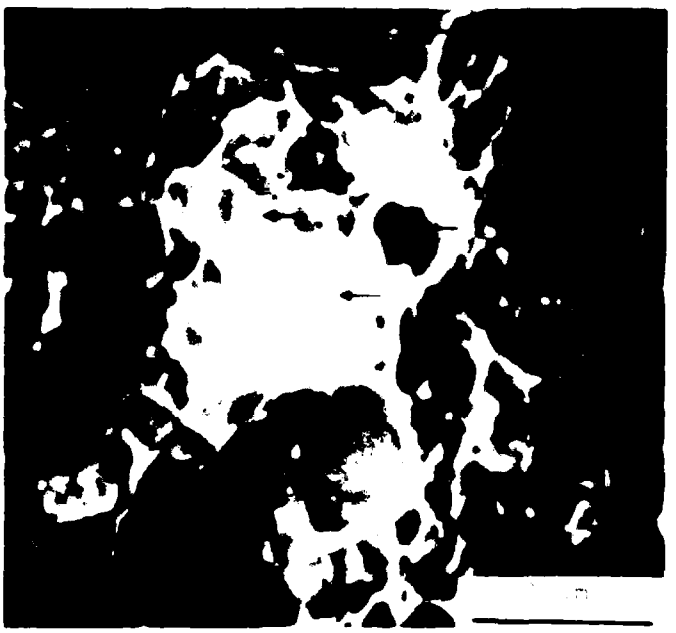

(b)

Figure 6. Fracture surfaces of Al-8Fe-7Ce: (a) small dimples mixed with large cavities, and (b) small dispersoids in shallow dimples.

Zone A particles in which the fracture process, as shown in Fig. 7a, is characterized by void nucleation and coalescence at small dispersoids located near the Zone A particles. This type of fracture results in protrusions in one-half of the specimens with matching cavities in the other, and is consistent with the observation of 5-10 μm diameter dimple-covered cavities on the fracture surface in Fig. 6a. Fracture at or near the interface of Zone A particles was also observed in Al-8Fe-7Ce tested at elevated temperatures (150-230°C) [7].

The size of the dimples in the three Al alloys is less than 2 μm in diameter. Examined with stereo pairs, the dimples appeared to be quite shallow. In many cases, small dispersoids of 0.2-0.5 μm diameter were found at the bottom of the dimples (Fig. 6b). Several areas of the Al-Fe-V alloy showed powder particle pull-out, indicating inadequate strength of extruded powder particle boundaries (Fig. 7b). In the Al-Fe-Mo-V CT specimens, spherical, unfractured particles of 10-20 μm diameter were found to debond along the particle/matrix interface. Auger and EDS analyses revealed that they are Al-Fe-Mo-V particles with Ti on the surface. Also observed in a previous investigation [3], these particles are few in number, widely spaced, and do not appear to be the controlling fracture mechanism or responsible for the low fracture toughness of Al-8Fe-2Mo-1V. Instead, preliminary results indicate that the controlling fracture mechanism in Al-Fe-X alloys appears to be cavity nucleation at 0.1-1 μm diameter dispersoids. Fracture at prior powder particle boundaries is also a possibility but further work is required to verify this fracture mode.

e. Discussion on Toughness Enhancement and Future Work

It appears that several steps can be considered as possible means for improving the fracture toughness of Al-Fe-X alloys. These potential toughness-enhancement measures are:

(1) elimination of large, extraneous particles such as Al-Fe intermetallics and stringer inclusions from the microstructures;

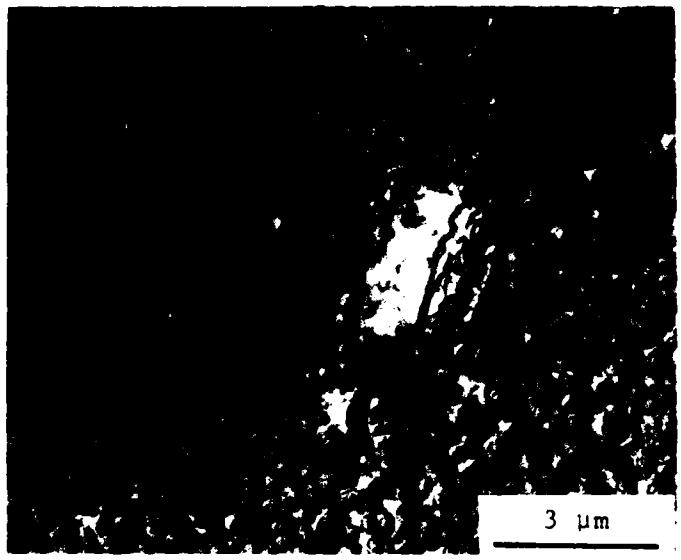

(a)

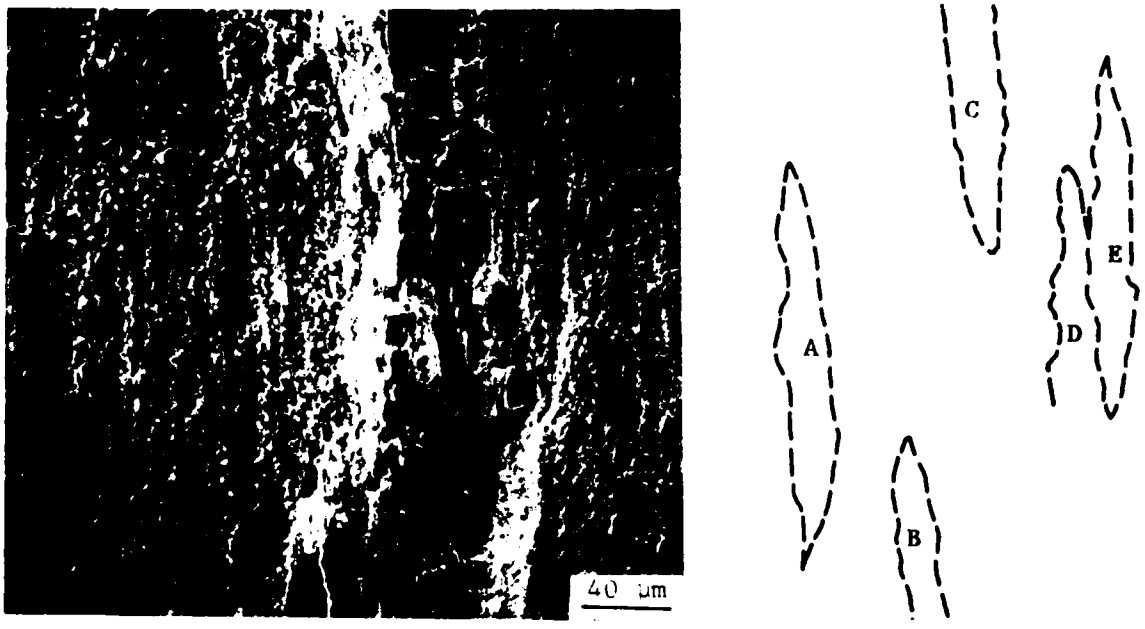

(b)

Figure 7. Fracture mechanisms in Al-Fe-X alloys: (a) void nucleation at dispersoids located near a Zone A particle in Al-8Fe-7Ce, and (b) fracture along prior powder particle boundaries in Al-10Fe-2.5V.

(2) reduction of dispersoid size to less than 0.01 μm diameter as a means for increasing the critical strain to cavity nucleation [8,9];

(3) improving prior powder particle boundary strength by modifying the powder processing technique or the hot extrusion procedures (see, e.g. [10]).

These preliminary suggestions will serve as the directions for future work in this program. Researchers at Allied-Signal Corporation have recently developed a series of Al-Fe-V-Si alloys which show higher K_{Ic} values than those investigated in the present program [11,12]. The fracture behavior of one particular Al-Fe-V-Si alloy (Al-8Fe-1.5V-1.5Si) will be examined and compared with those of the Al-Fe-Ce and Al-Fe-Mo-V alloys in the coming year.

3. References

[1] S. L. Langenbeck et al., Elevated Temperature Aluminum Alloy Development, Final Report, AFWAL-TR-86-4027, 1986.

[2] H. Jones, Mater. Sci. and Eng., Vol. 5, p. 1, 1969-70.

[3] R. A. Rainen et al., Elevated Temperature Aluminum Alloy Development, Interim Tech. Report (LR30903), Air Force Contract F33615-81-C-5096, 1985.

[4] ASTM E-399; Annual Book of ASTM Standard, ASTM, Philadelphia, PA, pp. 547-582, 1985.

[5] C. Q. Chen and J. F. Knott, Metal Science, Vol. 15, pp. 357-364, 1981.

[6] G. G. Garrett and J. F. Knott, Met. Trans. A., Vol.9A, pp. 1187-1201, 1978.

[7] S. L. Langenbeck et al., Elevated Temperature Aluminum Alloy Development, Interim Tech. Report (LR 30662), Air Force Contract F33615-81-C-5096, 1984.

[8] K. Tanaka, T. Mori, and T. Nakamura, Phil. Mag., Vol. 21, pp. 267-279, 1970.

[9] A. S. Argon, J. Im, and R. Safoglu, Met. Trans., Vol 6A, pp. 825-837, 1975.

[10] E. Lavernia, G. Rai, and N. J. Grant, Mat. Sci. and Eng., Vol. 79, pp. 211-221, 1986.

[11] A. M. Brown, D. J. Skinner, D. Raybould, S. K. Das, R. L. Bye, and C. M. Adams, Int. Conf. on Aluminum Alloy, Charlottesville, VA, June 15-20, 1986.

[12] D. J. Skinner, R. L. Bye, D. Raybould, and A. M. Brown, Scripta Met., Vol. 20, pp. 867-872, 1986.

III. PUBLICATIONS (AFOSR SPONSORSHIP)

A. Task 1. Crack Tip Micromechanisms and Fatigue Lifetime Prediction

1. "The Distribution of Strain Within Crack Tip Plastic Zones" - D. L. Davidson, Engineering Fracture Mechanics 25, 123-132, 1986.

2. "The Breakdown of Crack Tip Microstructure During Fatigue Crack Extension" - D. L. Davidson and J. Lankford in High Strength Powder Metallurgy Aluminum Alloys - II, G. J. Hildeman and M. J. Koczak, eds., TMS-AIME, Warrenville, PA, 1986, pp. 47-59.

3.* "Plasticity Induced Fatigue Crack Closure" - D. L. Davidson, ASTM Fatigue Crack Closure Conference Proceedings.

4.* "Local Crack Tip Opening Load and Its Dependence on Fatigue Loading Variables" - S. J. Hudak and D. L. Davidson, ASTM Fatigue Crack Closure Conference Proceedings.

---

*Manuscripts prepared during the year, but not yet published.

IV. PROGRAM PERSONNEL

Name	Title	
Dr. James Lankford	Institute Scientist	Co-Principal Investigators
Dr. David L. Davidson	Institute Scientist	
Dr. Gerald R. Leverant	Director, Materials Sciences	
Dr. K. S. Chan	Senior Research Engineer	
Mr. Harold Saldana	Staff Technician	
Mr. John Campbell	Senior Technician	
Mr. James Spencer	Senior Technician	

V. INTERACTIONS - 1986

A. Task 1. Crack Tip Micromechanisms and Fatigue Lifetime Prediction

1. Interaction with many investigators, both U.S. and foreign, at the Engineering Foundation Symposium on Small Fatigue Cracks.

2. Presentation of paper at ASTM Symposium on Fatigue Crack Closure, Charleston, SC, "Plasticity Induced Fatigue Crack Closure", D. L. Davidson.

3. Presentation of work and interaction at NSF Workshop on Fracture of Rock and Rock Mechanics, Park City, UT, D. L. Davidson.

4. Presentation of paper at Southwest Research Institute Workshop on "Development of Fatigue Crack Tip Deformation Models" by D. L. Davidson; outside participants: C. Atkinson, D. M. Barnett, W. W. Gerberich, M. Denda, J. C. M. Li, J. C. Newman, Robb Thomson.

5. Presentation of paper at TMS Meeting, Orlando, FL, "A Computer Simulation of Fatigue Crack Growth", D. L. Davidson.

B. Task 2. Microstructure/Property Relationships in Advanced Structural Alloys

1. A paper entitled, "Fracture of Dispersoid-Strengthened Aluminum Alloys," by K. S. Chan and G. R. Leverant, to be presented at the 1987 TMS Annual Meeting at Denver, CO, Feb. 24-27, 1987.

2. A paper entitled, "Fracture Toughness of Dispersoid-Hardened Aluminum Alloys," by K. S. Chan and G. R. Leverant, to be presented at WESTEC 87, Los Angeles, CA, March 23-26, 1987.

END

5-87

DTIC